Locking strategy for the Advanced Virgo Central Interferometer

VIR-0187A-16

A. Allocca[1,2,*], A. Chiummo[3], and M. Mantovani[3]

[1]*Università di Pisa*
[2]*INFN - Sezione di Pisa*
[3]*EGO - European Gravitational Observatory*

Date: April 28, 2016

[*] *corresponding author:* allocca@pi.infn.it

Contents

1 Introduction

In this note the control strategies for the Central Interferometer will be investigated, with particular attention to the alignment sensitivity of the error signals. In particular, more than identifying the locking strategy, the critical issues of the Recycling Cavity due to its low Gouy phase will be highlighted, and possible alternatives to overcome this problem will be presented.

The Central Interferometer (CITF) is composed of four main optics: the Power Recycling mirror (PR), the Beam Splitter (BS) and the West and North Input mirrors (WI and NI, respectively). Moreover, along the beam path, three additional optics can be found: the Compensation Plates (CP), which are put on the back side of the Input Mirrors and are used to perform the Thermal Compensation of mirror defects, and the Pick-Off Plate (POP), which is used to extract a pick-off beam from the cavity and is placed in front of the Power Recycling mirror. A schematic of the CITF is reported in figure 1.

The locking of the CITF involves the control of two different degrees of freedom: one is the length of the Power Recycling Cavity (PRC), which is called PRCL: this cavity is composed of the PR mirror as *input* mirror and the compound mirror NI-BS-WI as *end* mirror. The second length to control is the asymmetry of the Michelson short arms, said MICH, which affects the reflectivity of the PRC end mirror for the sidebands. Referring to figure 1, these lengths are defined as:

$$\text{PRCL} \quad = \quad l_{PR} + \left(\frac{l_{NI} + l_{WI}}{2} \right) \tag{1.1}$$

$$\text{MICH} \quad = \quad |l_{NI} - l_{WI}| \tag{1.2}$$

The control is performed through the usual PDH technique [1].
In this note, it will be analyzed the case in which error signals are extracted through a photodiode in reflection of the PRC, called B2, which has been installed as first.
To actuate on the two degrees of freedom, the driving matrix shown in table 1 is used.

In order to have a good control of each degree of freedom, it is necessary to choose the best combination of signals which diagonalizes the sensing matrix: in other words, we need the two signals used to control PRCL
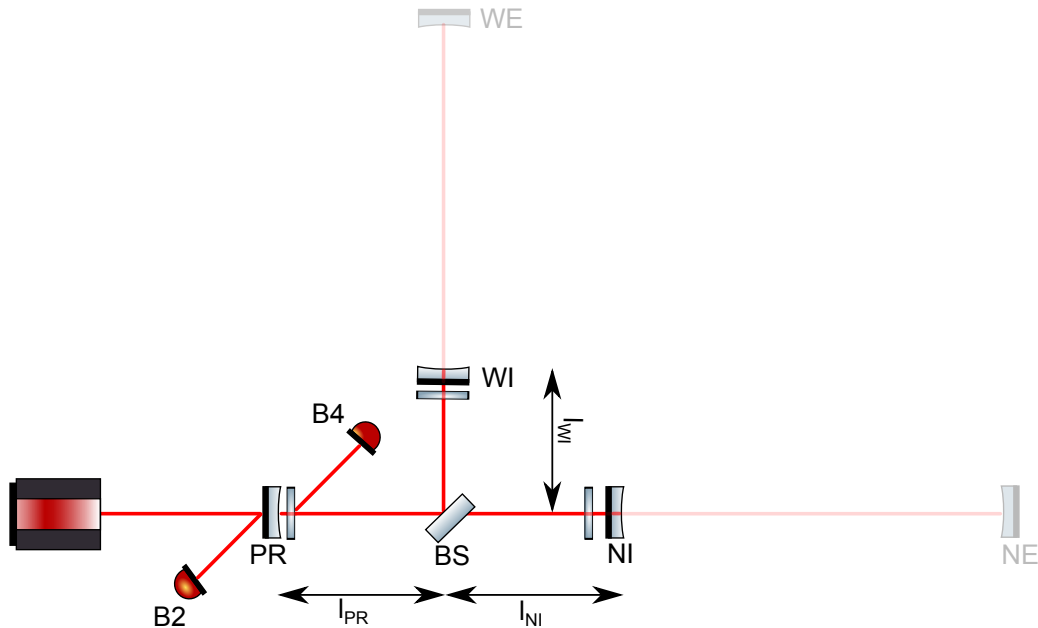
Figure 1: Schematic of the central interferometer. Arm cavities are shown as semi-transparent.

	NI	WI	BS	PR
PRCL	0	0	0	1
MICH	1	-1	0	0

Table 1: Driving matrix for the two degrees of freedom of the CITF. On the first line, the names of the mirrors are reported (in order): North Input (NI), West Input (WI), Beam Splitter (BS) and Power Recycling (PR).

and MICH to be well decoupled from each other. In general, the choice of the best optical sensing matrix relies also on a high SNR. However, since the noise curves of the detector were not available when this study has been performed, this aspect will not be evaluated throughout this note.

The main aspect which is investigated in this work is the robustness of the error signals to the misalignments.

Power Recycling Cavity stability

The Power Recycling Cavity (PRC) in Advanced Virgo is designed as a *marginally stable* cavity: indeed, the cavity Gouy phase is about 2 mrad, which brings the cavity very close to the instability condition. The net effect is that any difference with respect to the ideal conditions strongly affects the error signals optical gains and shapes. This situation results to be even more difficult with respect to the case of Virgo+, where the Recycling Cavity Gouy phase was about 9 mrad.

In order to make the lock of CITF easier, it has been investigated the possibility of increasing the stability of the Recycling Cavity by acting on the mirrors Radii of Curvature using the Thermal Compensation System (TCS) [2]. This is made possible thanks to the *Ring Heaters* (RH), which surround all the main optics (except for the BS), and are intended to decrease the mirrors radius of curvature. Moreover, thanks to the *Central Heating*, a Gaussian CO_2 beam which acts on the two Compensation Plates, it is also possible to increase the Radius of Curvature of the Input Test Masses.

In this work, it has been explored the possibility of increasing the cavity Gouy phase with respect to the nominal value using only the RH surrounding the PR (which has been installed as first) in order to get closer to the Virgo+ conditions. This strategy has the drawback of introducing of a mismatch between the recycling cavity mode and the input beam mode, which might not be compensated with the input mode matching telescope.

Therefore, the aim of these simulations is to verify whether the overall effect of such Gouy phase increase is to enhance the cavity controllability.

2 CITF with nominal stability conditions

The operating point of the CITF is set in such a way the 6 MHz, 56 MHz and 131 MHz sidebands are resonating in the recycling cavity. In this configuration, the carrier is anti-resonant, and the 8 MHz sideband is almost completely reflected.

Hereafter, it will be studied the degradation of the error signal as a function of the cavity misalignment. In particular, the PR mirror will be misaligned by an angle ranging between 0 and 3 μrad in 20 steps, and the signal robustness will be evaluated by looking at the variation of the following as parameters:

- **Optical Gain**: this is the slope of the error signal at the working point or, equivalently, the low frequency limit of the transfer function between the Degree of Freedom and the photodiode signal. It is important to have the lowest possible Optical Gain variation with the misalignment: the smaller is the variation, the more robust is the signal choice.

- **Demodulation phase**: the demodulation phase adjustment allows to have the maximum signal either in phase ($\mathbf{p}$) or in quadrature ($\mathbf{q}$) in the PDH signal. Conventionally, the signal in $\mathbf{p}$ is used, while the one in $\mathbf{q}$ is discarded. If the demodulation phase gets too much affected by the misalignment, there is the risk to mix the p and q components and, therefore, to introduce unwanted couplings between the degrees of freedom during the alignment phase. Moreover, it also implies a loss of signal amplitude and optical gain.

- **Working point**: the Working Point is the zero crossing of the error signal. It might change with the alignment and, as for the demodulation phase, it is preferable to keep this change as small as possible in order to stay within the range of actuation on the mirrors and keep them in place.

- ***Quality parameter*** [3]: this parameter gives an indication about the separation between the signals used to control the CITF degrees of freedom, therefore it represents an indication of how good the signal combination is. Also in this case, the robustness of the control strategy translates in a high value and a small change of the quality parameter with the misalignment.

2.1 Error signal change as a function of the misalignments

In this section, the error signals demodulated at 6 MHz, 56 MHz and 131 MHz obtained for MICH and PRCL will be considered. The demodulation phase is optimized in such a way to have all the signal in p when there is a perfect alignment. Therefore, the PRM is misaligned, and the variation of demodulation phase, working point and optical gain is evaluated. In particular, starting from the error signal, a fit of the linear region around the zero crossing is performed, which allows to extract the slope (which represents the Optical Gain), the zero crossing (Working Point), and the demodulation phase, which is optimized as explained before.
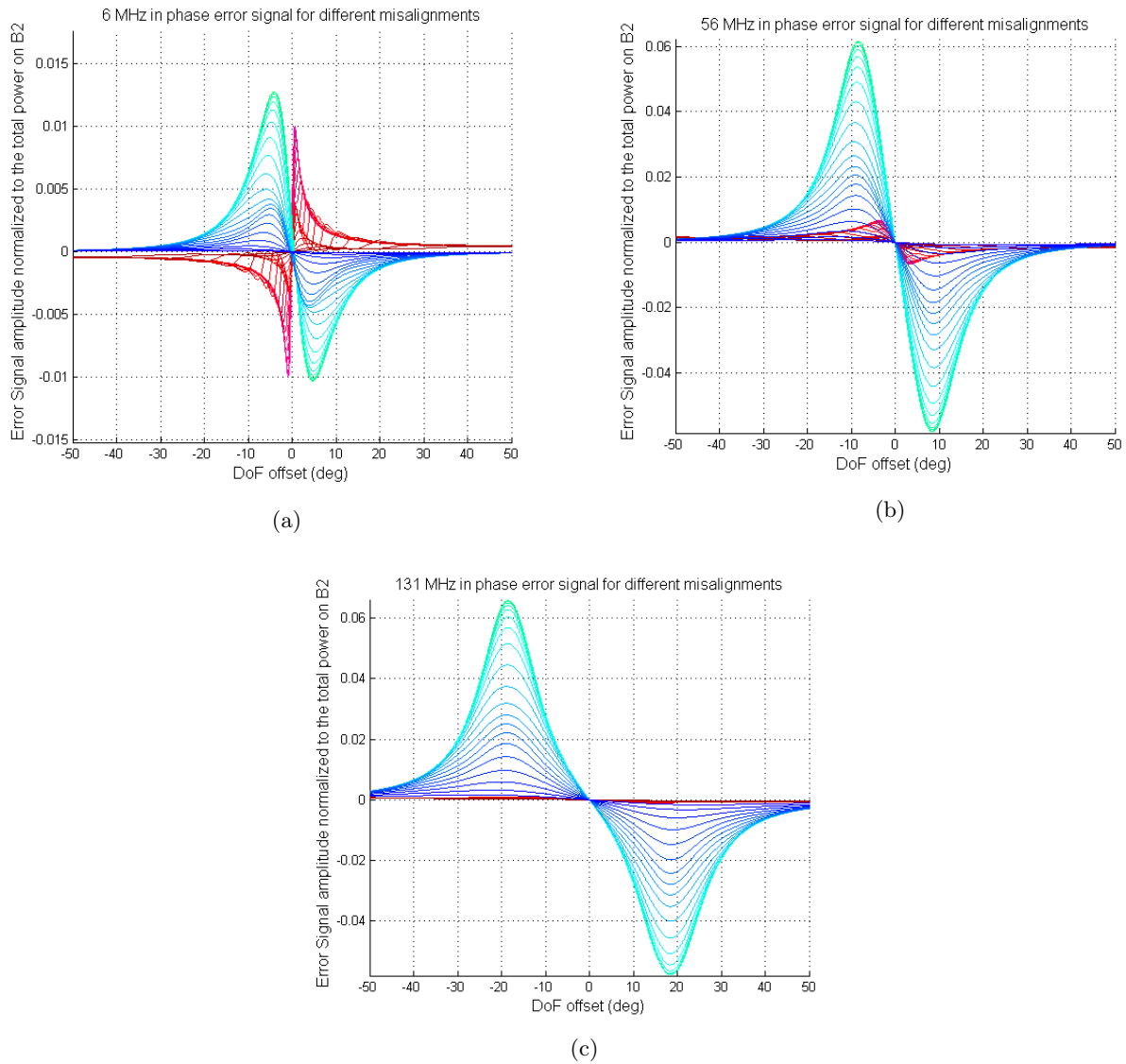
(a)

(b)

(c)

Figure 2: Error signal demodulated at 6MHz (a), 56 MHz (b) and 131 MHz (c) for different values of PR angular misalignment. The demodulation phase is optimized for MICH. The red-scale curves correspond to the PRCL degree of freedom, while the blue-scale curves correspond to MICH. The colorscale ranges from light red (green for MICH) for no misalignment to dark red (blue for MICH) for higher misalignments.
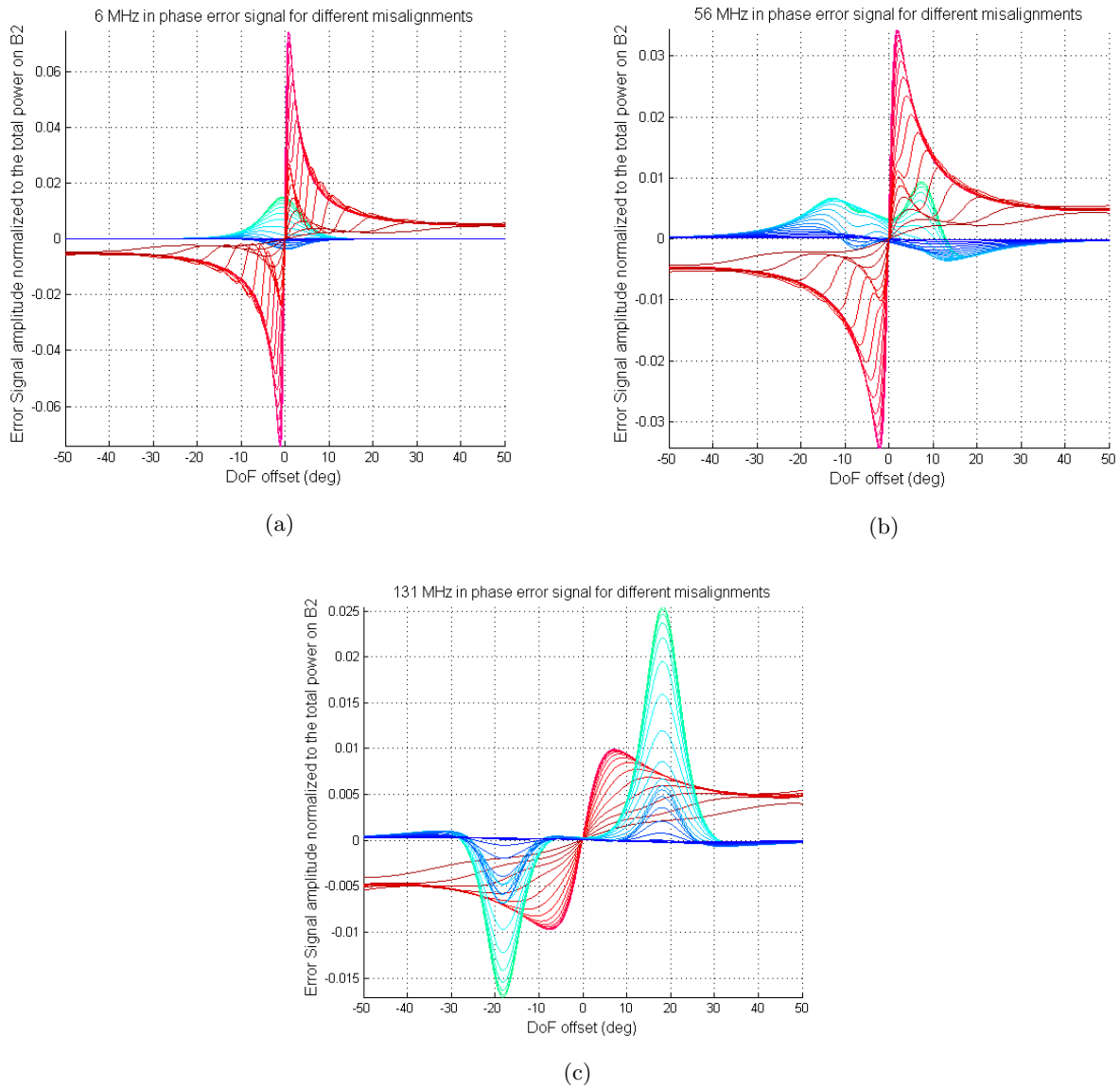
Figure 3: Error signal demodulated at 6MHz (a), 56 MHz (b) and 131 MHz (c) for different values of PR angular misalignment. The demodulation phase is optimized for PRCL. The red-scale curves correspond to the PRCL degree of freedom, while the blue-scale curves correspond to MICH. The colorscale ranges from light red (green for MICH) for no misalignment to dark red (blue for MICH) for higher misalignments.

2.1.1 Demodulation phase and working point variation with the misalignment

Say ϕ_0 the optimal demodulation phase which maximizes the signal in **p** for one selected degree of freedom. For each step of misalignment the optimal value of the demodulation phase is calculated, and the difference with respect to ϕ_0 is shown in figure 4, where the phase is optimized for MICH (left) and for PRCL (right) degree of freedom. As already mentioned, a variation of the demodulation phase corresponds to a mixing between the **p** and **q** components (which are 90 degrees apart), and therefore a coupling between the degrees of freedom and a reduction of the signal amplitude. However, as long as **p** and **q** do not mix a lot, this variation is not considered to be worrying.

As shown in the plots, the highest demodulation phase variation with the misalignment is about 15 degrees, and only happens for the 56 MHz: this variation does not involve a big mixing of **p** and **q** signals, so it can be considered to be acceptable.
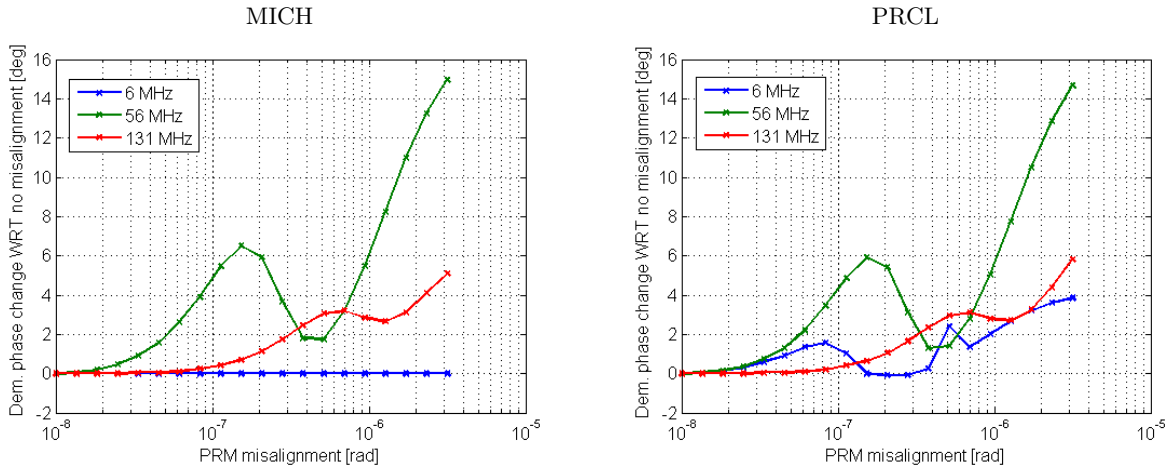

Figure 4: Demodulation phase optimized for the MICH (left plot) and PRCL (right plot) degrees of freedom as a function of the PRM misalignment. The three curves correspond to the 6 HMz (blue), 56 MHz (green) and 131 MHz (red). Notice that the demodulation phase variation of the 6 MHz sideband for MICH is always equal to zero because the signal is already all in p.

In figure 5 the variation of the working point with the cavity misalignment when the demodulation phase is optimized for MICH (left) and for PRCL (right) is shown. In this case, the highest working point variation is of the order of about 1 degree for MICH and 0.3 degrees for PRCL which correspond to 3 nm and 1 nm ($x_{[m]} = x_{[deg]} * \lambda/360$), respectively. This variation results to be within the range of the actuators used to keep the mirrors in the working position.
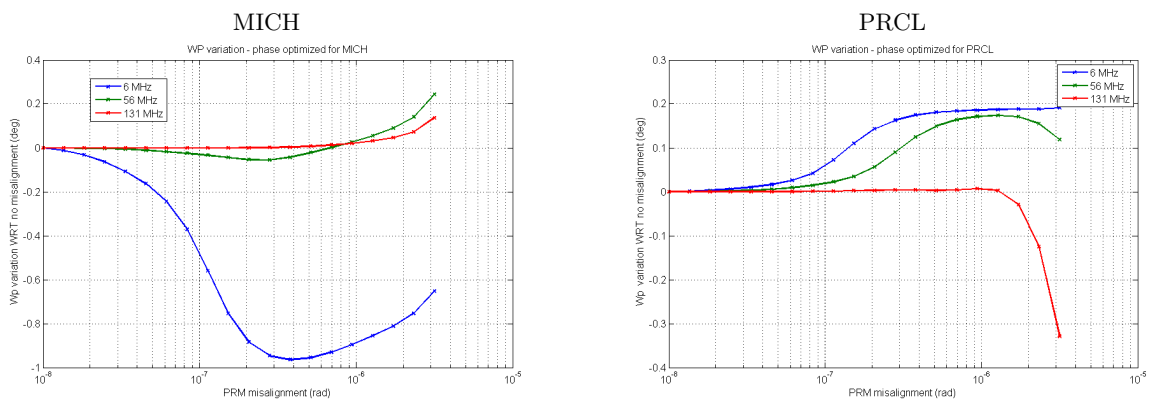
MICH

PRCL

Figure 5: Working point change as a function of the PRM misaligment for MICH (left) and PRCL (right).

2.1.2 Optical gain variation with the misalignment

Figure 6 shows the Optical Gain (OG) variation as a function of the PRC misalignment, normalized to the value of the OG for a perfect alignment.
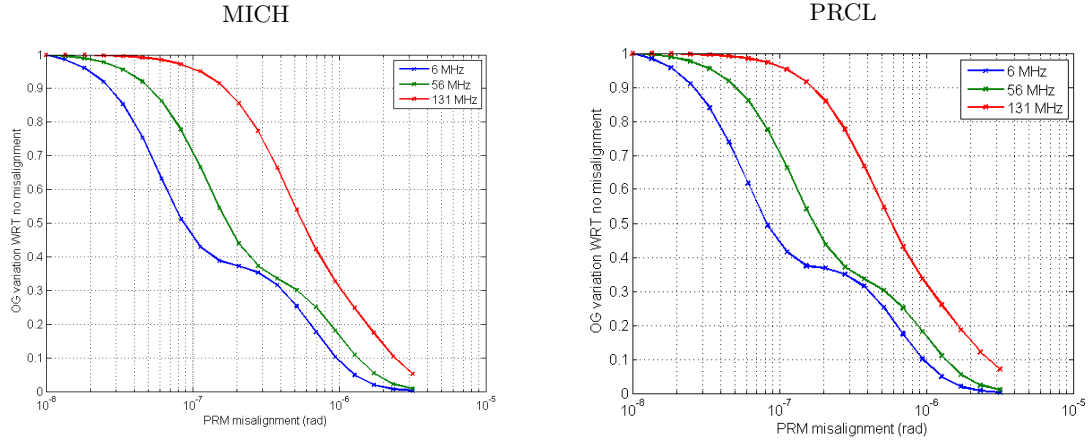

Figure 6: Optical gain variation for MICH (left) and for PRCL (right) as a function of the PRM misalignment. The value of the OG is normalized with respect to no misalignment.
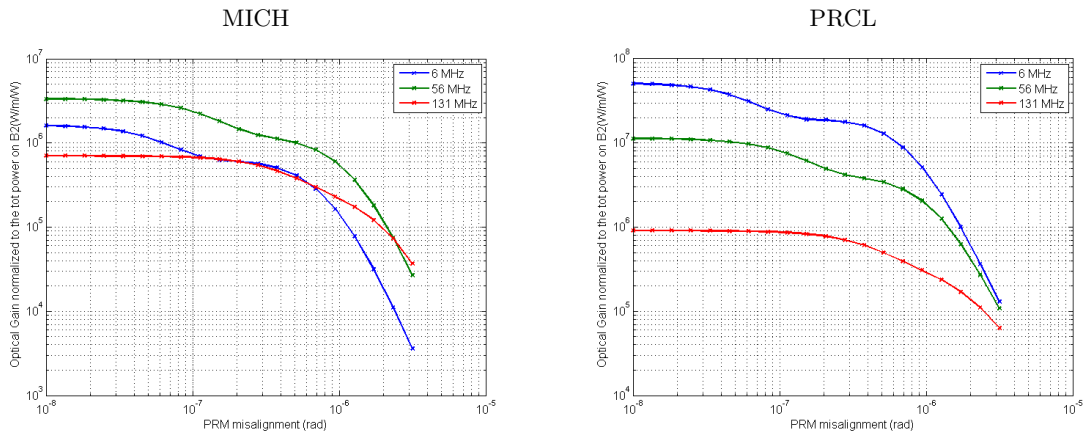

Figure 7: Absolute value of the optical gain for MICH (left) and for PRCL (right) as a function of the PRM misalignment.

For both the degrees of freedom, the higher is the finesse of the sideband, the higher is the sensitivity to the misalignments. Indeed, when the carrier is anti-resonant and the sidebands are resonant in the cavity, the recycling gain of the sidebands is given by:

$$\mathcal{G}_\Omega = \left(\frac{t_{PR}}{1 - r_{PR} cos\left(\frac{\Omega\Delta}{c}\right)} \right)^2 \tag{2.1}$$

where t_{PR} and r_{PR} are the transmissivity and the reflectivity of the power recycling mirror, respectively, Ω is the sideband modulation frequency and Δ is the Schnupp asymmetry. The recycling gain $\mathcal{G}$ and the finesse ($\mathcal{F} = \pi\mathcal{G}/2$) for the different sidebands are reported in table 2.

The link between Sideband Recycling gain and sensitivity to the cavity aberrations is confirmed by the fact that the OG of the 6 MHz signal drops at 40 % of the initial value after 0.1 mrad of PRM misalignment. On the

Sideband frequency	Recycling Gain	Finesse
6 MHz	48	75
56 MHz	10	17
131 MHz	1	1.6

Table 2: Recycling gain of the different sideband frequencies.

other hand, the same loss happens for a misalignment which is about ten times bigger for the 131 MHz, which therefore results to be more robust with respect to cavity aberrations.

However, the drawback of using this error signal is that the OG absolute value is about two orders of magnitude lower than the one of the 6 MHz, as shown in figures 7 (a) and (b), where the absolute value of the optical gain is plotted against the cavity misalignment. Moreover, since the recycling gain of the 131 MHz is very low, also its amplitude results to be low which, probably, gives rise to a low SNR.

To better understand the behavior of the OG, the beam amplitude profile on the B2 photodiode has been studied at different modulation frequencies, as shown in figure 8. In figure 8a the beam shape for the 6 MHz sideband is plotted: it is no longer gaussian after a very small misalignment of 0.05 μrad. It explains the sudden drop of the OG. On the other hand, the smoother trend of the 131 MHz, shown in figure 8 (c), is explained by the fact that the beam shape is still gaussian up to a misalignment ten times bigger than for the 6 MHz, after which only its ellipticity is increased.
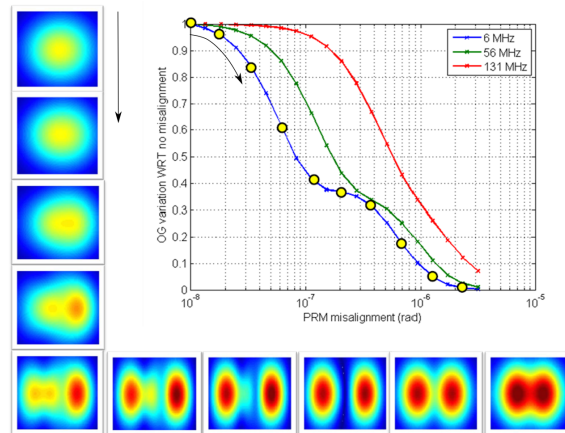
(a)
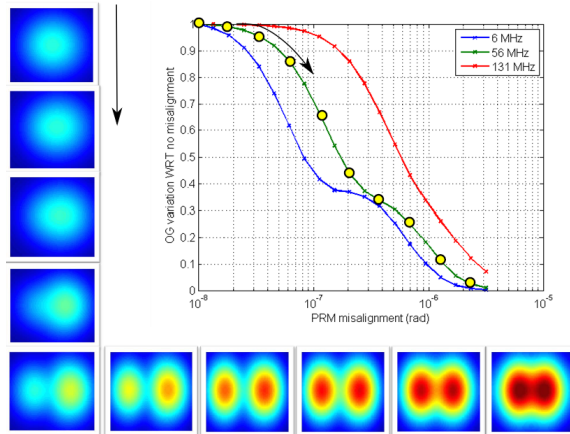
(b)
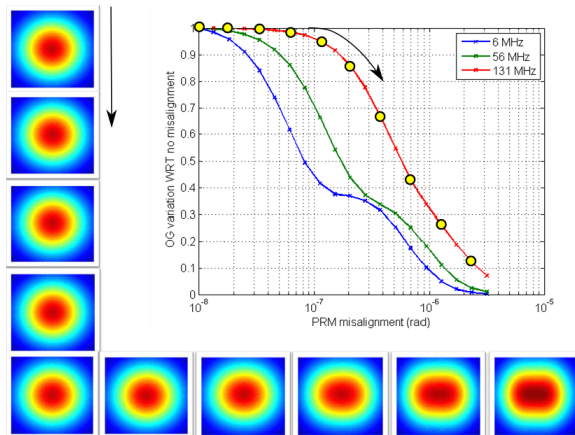
(c)

Figure 8: Beam profile of the 6 MHz (a), 56 MHz (b) and 131 MHz (c) sidebands as seen by the B2 photodiode for PRCL (a similar situation can be found also for MICH). In the squares all around the OG variation, from top-left to bottom-right, the beam amplitude profile is shown for increasing PRM misalignment, highlighted with the yellow dots in the plot of the OG variation. For the 6 and 56 MHz sidebands, the beam is no longer gaussian shaped already starting from less than 1 tenth of μrad of misalignment. It explains the sudden drop of Optical Gain to the 40 % of its initial value. On the other hand, PR misalignment does not affect strongly the 131 MHz beam shape: it translates into a smoother OG decrease.

2.2 Quality parameter variation with the misalignment

In order to find the best combinations of signal to control the two degrees of freedom, the *quality parameter* for each combination of signals has been evaluated. To give an idea of what this parameter is, here it is reported a brief summary from [3].

The *optical matrix* $\boldsymbol{M} = M_{ij}$ describes the photodiodes response s_i to the Degrees of Freedom change z_j:

$$M_{ij} z_j = s_i$$

In order to evaluate the controllability of a n-dimensional system, described by the optical matrix M with dimension $n \times n$, we can compute the reconstructed volume in the mirror space by using the wedge product as:

$$V = |det(M^{(N)})|$$

where V is the volume spawned by the normalized sensor signals in the mirror space.

This volume already provides information about the controllability of the system: 0 correspond to an uncontrollable system while 1 correspond to a perfectly decoupled system. Moreover, we can build a new equivalent (*iso-volumetric*) matrix constructed to have the first $(n-1)$ vectors being orthogonal and the n-th vector being misaligned with respect to the first vector by an angle α, which is the *quality parameter* and is defined as:

$$\alpha = \arcsin(|det(M)|) \tag{2.2}$$

This parameter ranges between 0 (no controllability) and 90 degrees (best controllability). Therefore, the higher α, the more decoupled the control.

In practice, this parameter is computed as following: the demodulation phase of each error signal is optimized for one degree of freedom per time. Then the optical gains are computed: in particular, the optical gain for PRCL and for MICH when the phase is optimized for PRCL, and the same when the demodulation phase is optimized for MICH. Finally, for each error signal choice a 2×2 matrix is built, as:

	PRCL	MICH
PRCL error signal	m_{11}	m_{12}
MICH error signal	m_{21}	m_{22}

The quality parameter α is given by the determinant of this matrix, having the row vector normalized, and there are as many matrices as many combination of signals are computed.

The robustness of the locking strategy with respect to the PR misalignment has been checked, and is shown in figure 9. While the matrix results to be diagonal for PRCL regardless of the signal choice, it is not the case for MICH, for which the best signal to use to achieve the control results to be the 131 MHz: indeed, in this case the parameter α results to be about 90 degrees.
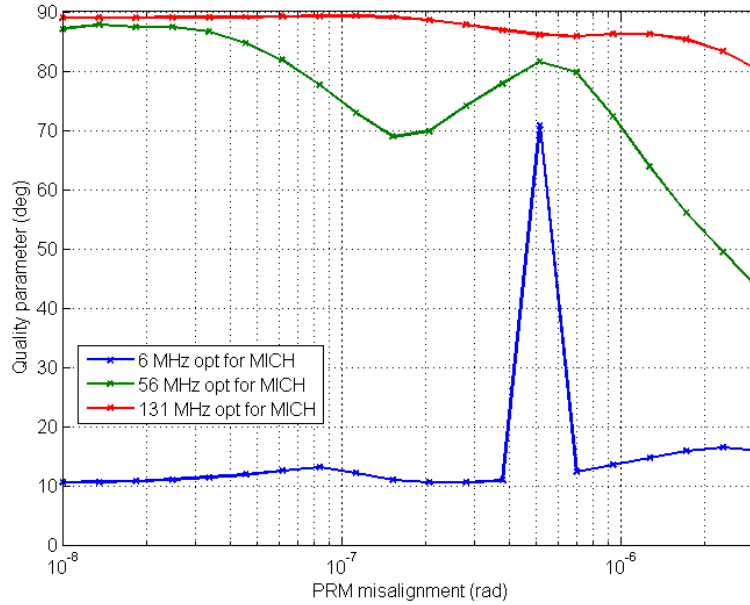
Figure 9: Variation of the quality parameter α with the PR misalignment. Regardless of the signal used to control PRCL, the robustness of the locking strategy is dominated by the signal choice for MICH. In particular, the best signal combination is obtained when MICH is controlled using the 131 MHz.

2.3   Conclusions

In this section the possible locking strategy of the CITF in nominal conditions using only one photodiode has been analyzed. The first conclusion from this study is that, for a perfect alignment, the 6 MHz and 56 MHz signals are good candidates to control the PRCL degree of freedom, while the best diagonalization is obtained with the 131 MHz for MICH. Nonetheless, the higher the signal finesse, the higher the sensitivity to cavity misalignments. For this reason, having the 131 MHz sideband to acquire the lock results to be crucial, since its Optical Gain drop results to be smoother than for the other frequencies.

However, since the amplitude of the signal is small and its Optical Gain is very low (as it is related to the Finesse), the SNR could not be sufficient to engage the control.

For this reason, in the next sections the possibility of increasing the cavity stability by varying the mirrors Radii of Curvature will explored.

3   Increasing the stability conditions

One of the main differences between Advanced Virgo and Virgo+ is related to the stability condition of the recycling cavity (see Appendix A for more details): indeed, because of a very small Gouy phase, higher order modes are brought into resonance even with very small cavity misalignments, and one of the main consequences of that is a degradation of the error signal and a drop of the optical gain.

A possibility to start closer to the conditions of Virgo+ is to take advantage of the Thermal Compensation System and change the mirrors Radii of Curvature with respect to the nominal value in order to improve the cavity stability and facilitate the alignment while keeping the lock. More in detail, in this note the possibility of varying the RoC only of the Power recycling mirror has been explored. The main drawback of this strategy is to introduce a mismatch between the input beam and the cavity mode. However, once the lock has been acquired and the alignment adjusted, it is possible to bring the radii of curvature back to the nominal conditions.

3.1 Cavity stability

In figure 10 it is shown the cavity Gouy phase as a function of the Radii of Curvature of Power Recycling (x axis) and Input (y axis) mirrors. The colorscale identifies different values of the cavity Gouy phase, therefore in the dark blue region the cavity is unstable. The white dot is the value of the Gouy phase for nominal Radii of Curvature in Advanced Virgo configuration.

Varying the RoCs while keeping the matching means moving along the line of constant Gouy phase. The black dashed-dotted line shows the region of the plot where the Gouy phase is equal to 9 mrad, which corresponds to the Gouy phase for the recycling cavity in V+.

In order to increase the cavity stability and evaluate the signals robustness, it has been simulated the situation in which the PRM and the Input mirrors RoCs are tuned in such a way to get a cavity Gouy phase very close to the V+ configuration. This condition can be achieved by using the Ring Heater to reduce the PRM RoC. The simulated condition is shown with a black star in figure 10.
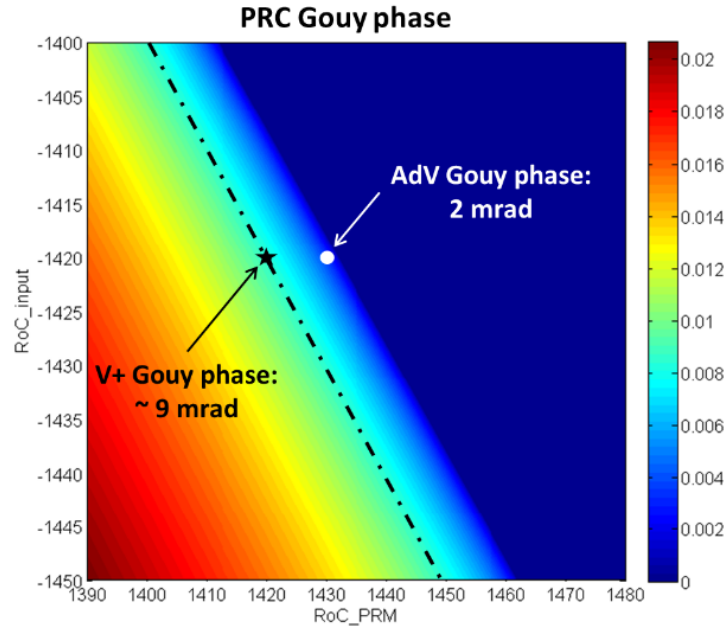

Figure 10: Gouy phase of the power recycling cavity as a function of the Power Recycling Mirror and Input mirrors Radii of curvature. Axes in meters, colorscale in radians.

3.2 Optical gain variation in a "more stable" recycling cavity

In this section it is analyzed the Optical Gain variation as a function of the PRC misalignment when its stability is increased to about the same value as in V+.

In figure 11 it is plotted the OG variation for the "more stable" (marked as *ms* in the legend) configuration. More specifically, for a higher cavity Gouy phase, the 6 MHz and the 56 MHz OG drop with the misalignment is less steep, while for the 131 MHz the situation is essentially unvaried (blue, green and red dashed lines, respectively).

To understand the origin of this improvement, the beam profile has been studied and is reported in figure 12. In particular, the profile of the 6 MHz sideband for the nominal stability condition (upper row) is compared

to the one for 8 mrad cavity Gouy phase (bottom row). In the latter case, the mismatch mode is visible, but the beam roundness is higher with respect to the lower stability condition case, and this gives rise to a higher robustness.

However, the absolute value of the OG reduces, as it is shown in figure 13: this is probably due to the introduced mismatch, which can also explain a lower value for the controllability, as shown in figure 14.
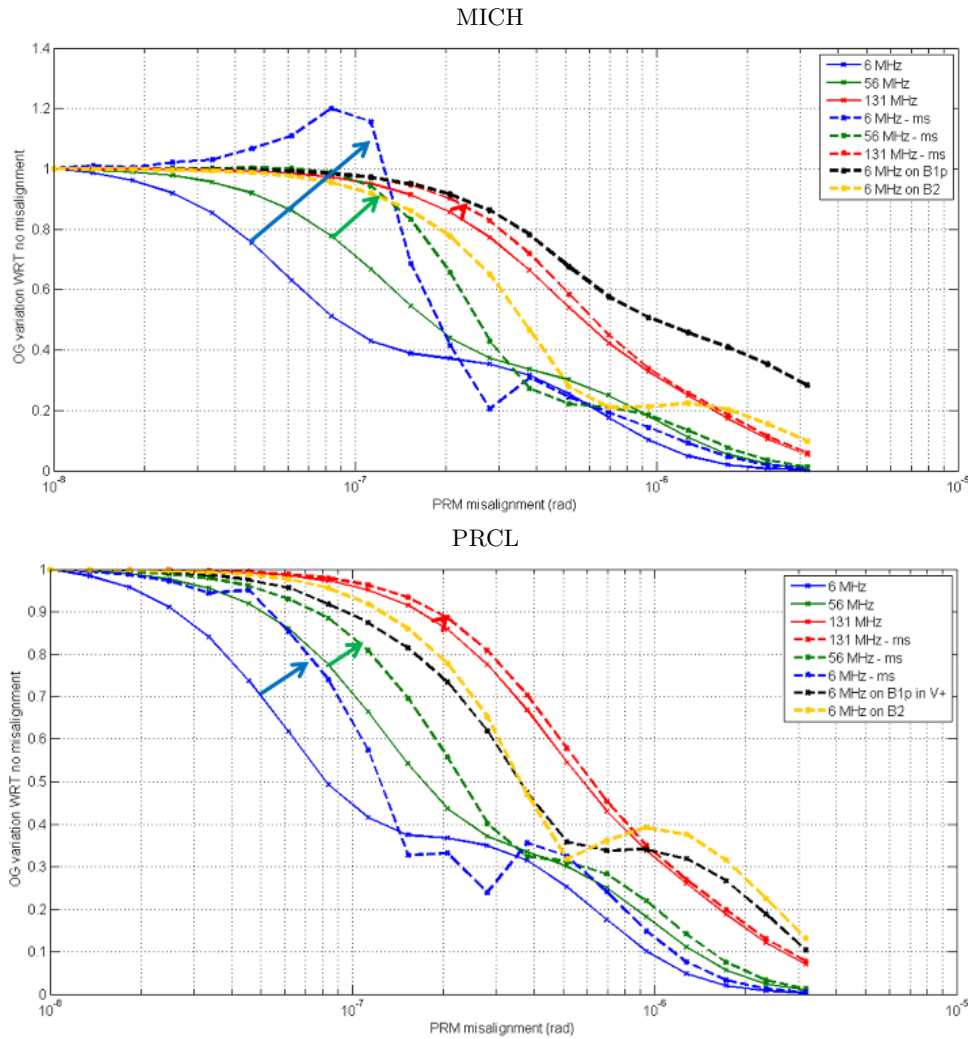

Figure 11: Optical gain change as a function of the misalignment for different cavity Gouy phase. For a higher Gouy phase, the optical gain drop is smoother for the 6 MHz and the 56 MHz (blue and green dashed lines, respectively), while it almost doesn't change for the 131 MHz (red dashed line). All the curves are compared to the situation in Virgo+ (yellow and black dashed lines).
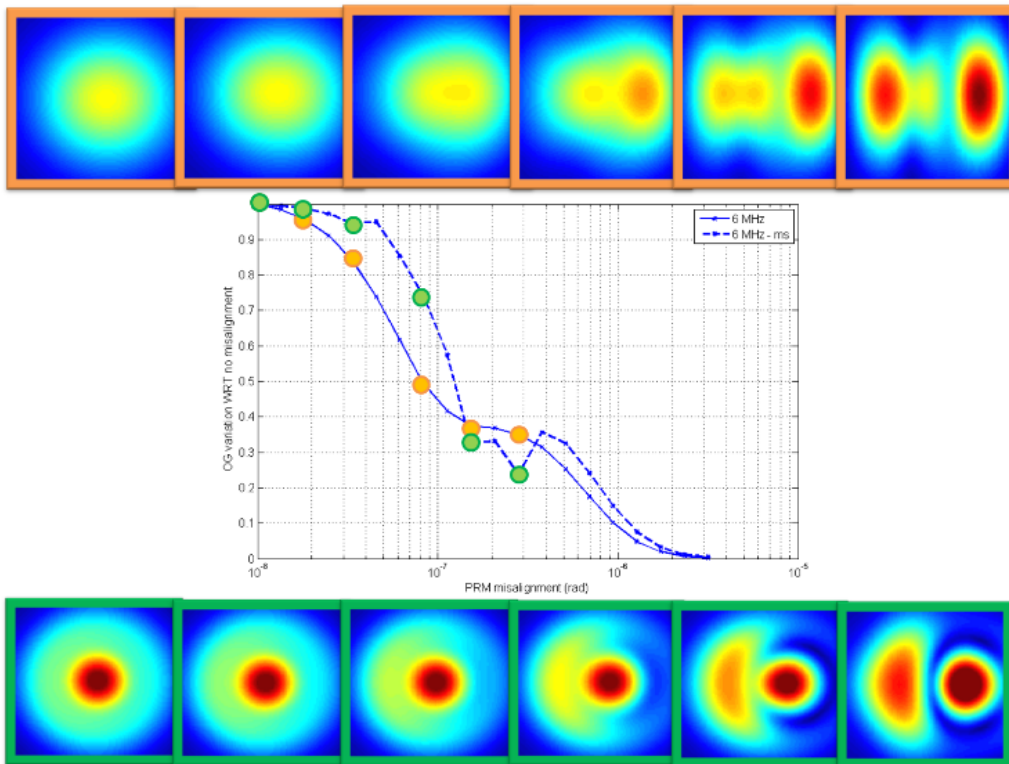
Figure 12: Beam profile of the reflected beam demodulated at 6 MHz. The beam profile for nominal cavity conditions (top) is compared to the beam obtained for increased cavity stability (bottom). From left to right, the images correspond to the dots on the curves, yellow for nominal and green for higher Gouy phase.
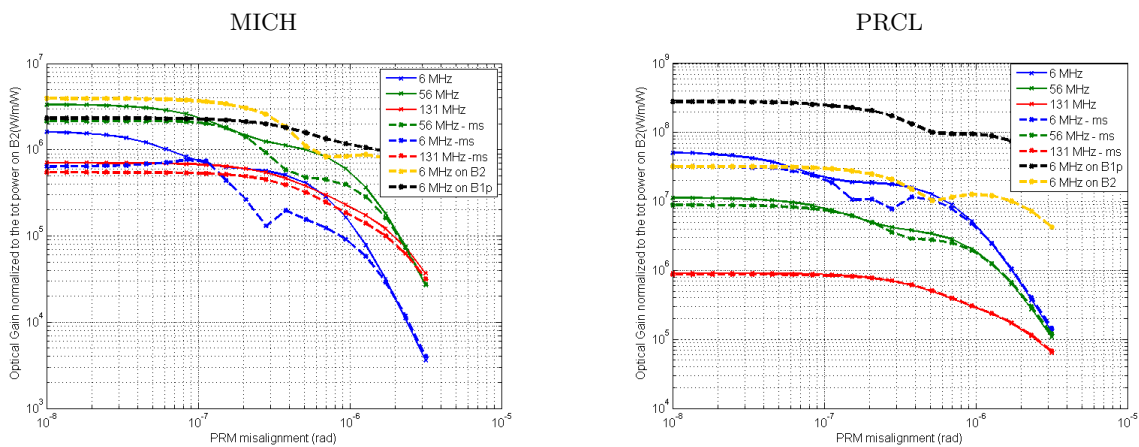

Figure 13: Absolute value of the Optical Gain as a function of the misalignment. The dashed blue, green and red lines correspond to the configuration of higher cavity stability. Because of the mismatch between the cavity mode and the input beam, the optical gain value is decreased.
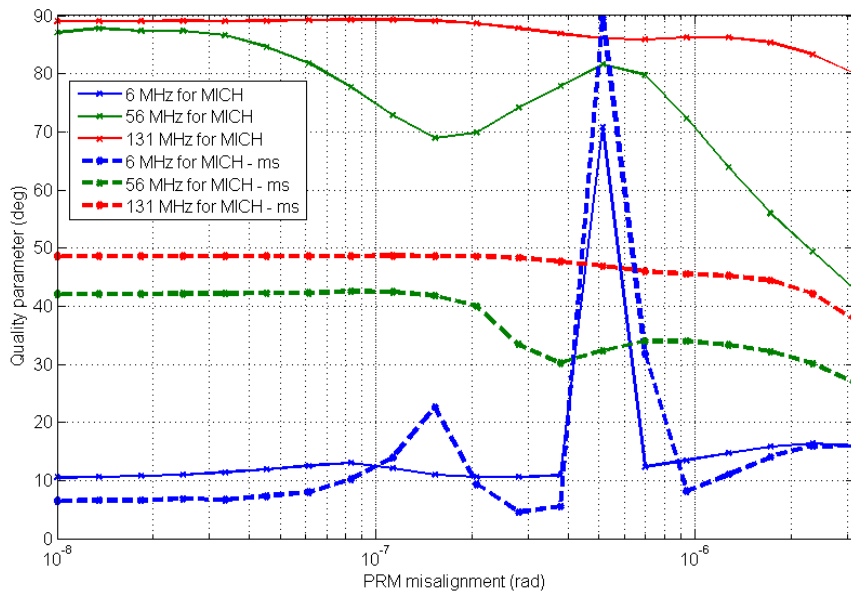
Figure 14: Quality parameter as a function of the misalignment for nominal conditions (continuous line) and increased cavity stability (dashed line).

4 Conclusions

Advanced Virgo has marginally stable Recycling Cavity, which makes the locking very sensitive to aberrations. In this note the locking strategy for the Central Interferometer has been investigated, using as only available photodiode the one in reflection of the Power Recycling Cavity (B2). In particular, the robustness of the error signals demodulated at 6 MHz, 56 MHz and 131 MHz has been checked against the cavity misalignments.

From this study it emerged that a deviation of the order of one tenth of microradiant from the ideal alignment conditions induces a deterioration of the error signal for the 6 MHz and 56 MHz frequency, unlike the 131 MHz which results to be more stable. This trend is explained by the sidebands recycling gain: indeed, the lower the finesse, the weaker the sensitivity to aberrations. Therefore, the use the 131 MHz becomes crucial, mostly for the control of the CITF differential degree of freedom (MICH).

However, because of its low recycling gain, the 131 MHz sideband has a very low amplitude, which could show a very low SNR, making it impossible to be used.

An additional possibility is to increase the cavity Gouy phase by changing the mirrors radii of curvature through the Thermal Compensation System: indeed, if on the one hand this solution introduces a mismatch, on the other hand the raise of the cavity stability allows for a higher robustness of the signals.

A   Comparison with Virgo+

In this section, a comparison between Virgo+ (V+) and Advanced Virgo (AdV) configurations is performed. The first aim is to cross-check the simulation results with experimental observation in V+. Moreover, this comparative study allows to better highlight the critical issues in AdV.

In V+ the locking was performed using the signal demodulated at 6.25 MHz. The main difference between AdV and V+ optical designs relies in the cavity Gouy phase, which is about 4 times smaller in AdV. In table 3 a comparison between V+ and AdV sidebdands Recycling Gain and PRC Gouy phase is reported.

	Modulation Frequency	Recycling Gain	PRC Gouy Phase
AdV	6.27 MHz	48	2 mrad
AdV	56 MHz	10	2 mrad
AdV	131 MHz	1	2 mrad
V+	6.25 MHz	30	9 mrad

Table 3: Recycling gain for the modulation frequencies of Advanced Virgo and Virgo +. The last column reports the Gouy phase for the Power Recycling Cavity.

In figure 15 it is displayed the Optical Gain variation for MICH and PRCL in AdV (already shown in figure 6) compared to the situation of Virgo+, represented with dashed lines. In particular, the yellow dashed curve refers to the signal demodulated at 6.25 MHz on B2 and the black dashed one is the signal demodulated at the same frequency, but extracted with the B1p photodiode (set at dark port). For both the signals, the Optical Gain variation with the cavity misalignment is comparable with the one of the 131 MHz for AdV. On the other hand, their absolute value is of the same order of magnitude as the 6 MHz for AdV.

This comparison points up the critical issues of the marginally stable recycling cavity in AdV, where a lower Gouy phase makes the signal demodulated at 6 MHz much more sensitive to cavity aberrations and therefore less robust.
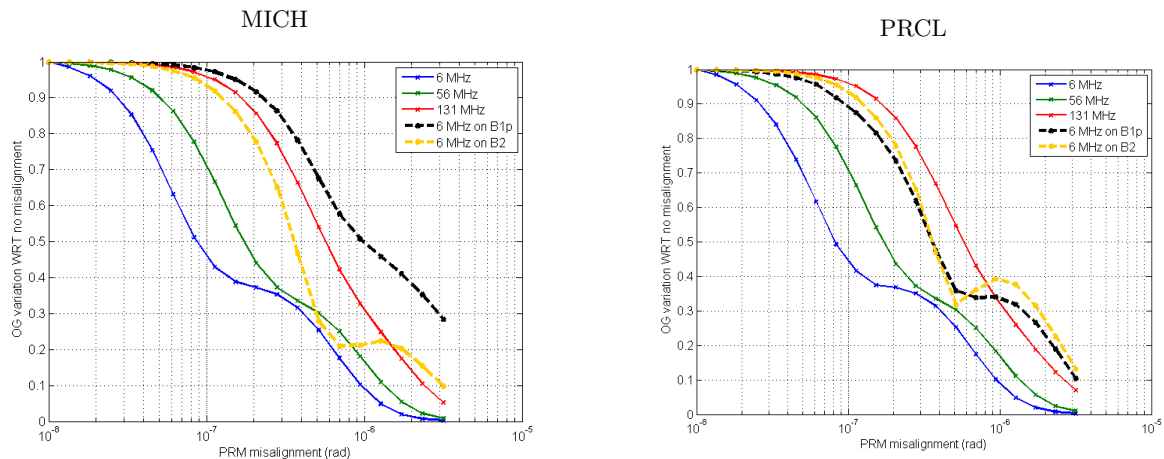

Figure 15: Optical gain variation for MICH (left) and for PRCL (right) as a function of the PRM misalignment. The value of the OG is normalized with respect to no misalignment. The black and the yellow dashed lines are the OG of the 6 MHz on B1p and on B2 computed for V+.
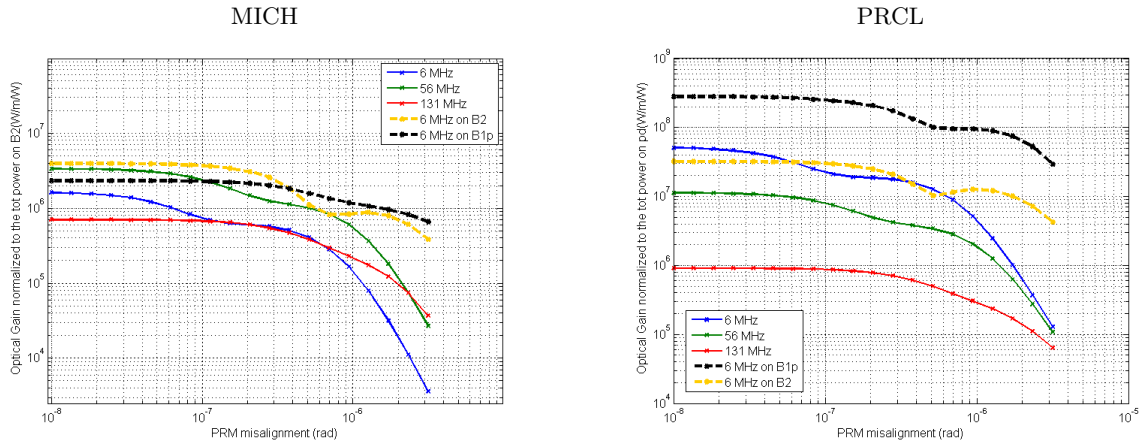
MICH   PRCL

Figure 16: Absolute value of the optical gain for MICH (left) and PRCL (right) as a function of the Power Recycling Mirror misalignment.

References

[1] R. W. P. Drever, J. I. Hall, F. V. Kowalski, J. Hough, G. M. Ford, A. J. Munley, H. Ward, *Laser phase and frequency stabilization using an optical resonator.* Appl Phys B 31 (2): 97 (1983). doi:10.1007/BF0070260 1

[2] The Virgo Collaboration, *Technical Documentation Report* (2012). 2

[3] M. Mantovani, A. Freise, *Evaluating mirror alignment systems using the optical sensing matrix.* 3, 11